

Cellular Senescence Promotes Skin Carcinogenesis through p38MAPK and p44/42MAPK Signaling

Fatouma Alimirah¹, Tanya Pulido¹, Alexis Valdovinos¹, Sena Alptekin^{1,2}, Emily Chang¹, Elijah Jones¹, Diego A. Diaz¹, Jose Flores¹, Michael C. Velarde^{1,3}, Marco Demaria^{1,4}, Albert R. Davalos¹, Christopher D. Wiley¹, Chandani Limbad¹, Pierre-Yves Desprez¹, and Judith Campisi^{1,5}



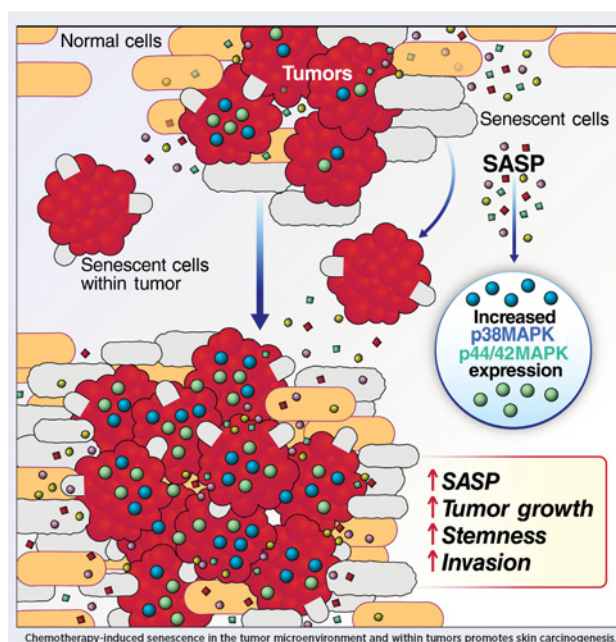
ABSTRACT

Cellular senescence entails an irreversible growth arrest that evolved in part to prevent cancer. Paradoxically, senescent cells secrete proinflammatory and growth-stimulatory molecules, termed the senescence-associated secretory phenotype (SASP), which is correlated with cancer cell proliferation in culture and xenograft models. However, at what tumor stage and how senescence and the SASP act on endogenous tumor growth *in vivo* is unknown. To understand the role of senescence in cancer etiology, we subjected p16-3MR transgenic mice, which permit the identification and selective elimination of senescent cells *in vivo*, to the well-established two-step protocol of squamous cell skin carcinoma, in which tumorigenesis is initiated by a carcinogen 7,12-dimethylbenz[α]anthracene, and then promoted by 12-O-tetradecanoyl-phorbol-13-acetate (TPA). We show that TPA promotes skin carcinogenesis by inducing senescence and a SASP. Systemic induction of senescence in nontumor-bearing p16-3MR mice using a chemotherapy followed by the two-step carcinogenesis protocol potentiated the conversion of benign papillomas to carcinomas by elevating p38MAPK and MAPK/ERK signaling. Ablation of senescent cells reduced p38MAPK and MAPK/ERK signaling, thereby preventing the progression of benign papillomas to carcinomas. Thus, we show for the first time that senescent cells are tumor promoters, not tumor initiators, and that they stimulate skin carcinogenesis by elevating p38MAPK and MAPK/ERK signaling. These findings pave the way for developing novel therapeutics against senescence-fueled cancers.

Significance: These findings identify chemotherapy-induced senescence as a culprit behind tumor promotion, suggesting that

elimination of senescent cells after chemotherapy may reduce occurrence of second cancers decades later.

Graphical Abstract: <http://cancerres.aacrjournals.org/content/cancerres/80/17/3606/F1.large.jpg>.



Introduction

Cellular senescence entails a permanent growth arrest wherein cells fail to proliferate but remain metabolically active. The senescence response is tumor suppressive and is established and maintained by pathways controlled by the p53 and p16^{INK4a} tumor suppressor proteins (1). This response is often triggered by potentially oncogenic stressors, and thus prevents stressed cells from progressing through the cell cycle and ultimately to malignancy (1). Among the stimuli that induce cellular senescence are mitochondrial dysfunction (2), telomere shortening (3), oncogene activation (4), epigenetic modifications (5), and genotoxic insults, including radiation and several anticancer agents (1).

Cellular senescence is paradoxical (6, 7). On the one hand, it is beneficial, optimizing certain steps in embryogenesis (8, 9), wound healing (6), and tissue reprogramming (7). On the other hand, despite protecting young organisms from cancer (1, 10), over time, senescent cells can evade the immune system and accumulate in tissues to secrete proinflammatory molecules, growth factors, and proteases to create a

¹Buck Institute for Research on Aging, Novato, California. ²Dokuz Eylul University School of Medicine, Izmir, Turkey. ³Institute of Biology, University of the Philippines Diliman, College of Science, Quezon City, Philippines. ⁴European Research Institute for the Biology of Ageing, University Medical Center Groningen, Groningen, the Netherlands. ⁵Biosciences Division, Lawrence Berkeley National Laboratory, Berkeley, California.

Note: Supplementary data for this article are available at Cancer Research Online (<http://cancerres.aacrjournals.org/>).

Corresponding Author: Judith Campisi, Buck Institute for Research on Aging, 8001 Redwood Boulevard, Novato, CA 94945. Phone: 415-209-2066; E-mail: jcampisi@buckinstitute.org

Cancer Res 2020;80:3606-19

doi: 10.1158/0008-5472.CAN-20-0108

©2020 American Association for Cancer Research.

procarcinogenic microenvironment (11). The senescent secretome, termed the senescence-associated secretory phenotype (SASP; ref. 11), is now recognized as a significant driver of many age-related pathologies (11, 12).

Recent studies show that the selective elimination of senescent cells using drugs (termed senolytics) or transgenic mice ameliorates many age-related phenotypes and diseases (12–14). Further, we used a transgenic mouse model (p16-3MR) to show that removing chemotherapy-induced senescent cells ameliorates several deleterious side effects of these therapies (15). In p16-3MR mice, the p16^{INK4a} (p16) promoter drives a herpes virus thymidine kinase (HSV-tk), which phosphorylates the nucleoside analog ganciclovir (GCV), converting it into a DNA chain terminator that fragments mitochondrial DNA (16), thereby inducing apoptosis selectively in p16-expressing senescent cells (6). However, how and at what stage senescent cells act on intrinsic tumor growth is not known.

A major side effect of genotoxic cancer treatments is an elevated risk of new neoplasms, unrelated to the primary cancer treated decades earlier (17). For example, childhood cancer survivors treated with radiation, which induces senescence (18), had a higher incidence of nonmelanoma skin cancer years after treatment for their original cancer (17).

Squamous cell skin carcinoma (SCC) develops from epidermal squamous cells, and is the second most prevalent type of nonmelanoma skin cancer (19). Unlike basal skin carcinoma, SCC has a higher rate of recurrence and metastasis (19). Indeed, patients with cancer treated with the genotoxic chemotherapeutic doxorubicin (DOXO) can develop SCC years after treatment (20, 21). DOXO, an anthracycline and topoisomerase II inhibitor, induces senescence and a SASP in cultured cells and mice (15). Thus, chemotherapy-induced senescence might contribute to SCC development *in vivo*.

To test this idea, we employed the well-established two-step skin carcinogenesis protocol to induce SCC (22). Following this protocol, we initiated tumorigenesis in p16-3MR mouse skin with a single dose of the DNA damaging carcinogen 7,12-dimethylbenz[α]anthracene (DMBA), followed by promotion with 12-O-tetradecanoyl-phorbol-13-acetate (TPA; ref. 22). DMBA causes H-Ras mutations, whereas TPA stimulates the growth of DMBA-initiated cells. This protocol leads to benign papillomas, which can eventually convert to carcinomas (22). We show for the first time that TPA, but not the single dose of DMBA, induces senescence and a SASP, suggesting that senescent cells might act as tumor promoters but not initiators. Multiple DMBA treatments also induce SCC (22), but the two-step protocol allowed us to determine whether senescent cells are tumor initiators or promoters. We also induced cellular senescence in p16-3MR mice using DOXO, then eliminated senescent cells with GCV followed by DMBA/TPA treatment. Senescent cells exacerbated tumor growth and the malignant conversion of benign tumors, whereas their ablation reduced tumor size and malignancy. Together, our findings provide a direct link between cellular senescence and cancer promotion *in vivo*, warranting the development of therapeutics against senescence-fueled cancers, including SCC.

Materials and Methods

Mice

p16-3MR mice were bred and housed at the Buck Institute for Research on Aging. All procedures were approved by the Institutional Animal Care and Use Committee. For all experiments, age-matched (3-month-old) p16-3MR homozygous female mice were randomly divided into experimental groups. Methods for senescence induction

and the two-step protocol in mice are in Supplementary Materials and Methods.

Cell lines and cell culture

Primary human neonatal keratinocytes (HEKn; ATCC PCS-200-010) from the ATCC, were maintained in dermal basal medium, Keratinocyte Growth Kit (ATCC) and antibiotics as per the manufacturer's instructions. A-431 (ATCC CRL1555) human epidermoid carcinoma cells from ATCC, were maintained in DMEM, 10% FBS (Thermo Fisher Scientific) and 0.01% penicillin/streptomycin (Corning). Cells were cultured in a 20% O₂, 5% CO₂ humidified incubator and were authenticated by ATCC, including short tandem repeat profiling. Primary HCA2 human foreskin fibroblasts were from O. Pereira-Smith (University of Texas Health Science Center, Houston, TX), and cultured in DMEM + FBS in a 3% O₂ incubator. They were not reauthenticated. Twenty-four hours prior to lysis, cells were cultured in supplement-free media. All cells were *Mycoplasma*-free.

Senescence induction in culture

DOXO hydrochloride from R&D Systems was dissolved in dimethyl sulfoxide (DMSO). Cells were treated with DMSO or DOXO at 250 nmol/L as described previously (15). We observed no cell death above the low background levels, and no reversal of senescence, as reported (23). For *in vivo* experiments, DOXO (2 mg/mL) was dissolved in warm endotoxin-free PBS (EMD Millipore). DMBA (2.5 mg/mL; Sigma-Aldrich) was prepared in acetone. TPA (Sigma-Aldrich) was prepared in acetone at 1.6 mmol/L or in DMSO at 100 μ mol/L for mouse and culture experiments, respectively. For TPA-induced senescence in culture, keratinocytes were treated with TPA (1.3–10 nmol/L) for 48 hours and maintained in TPA-free medium for an additional 10 days. TPA was dissolved in DMSO for cell culture experiments, and in acetone for mouse experiments, because low doses of acetone caused morphologic changes in cultured human keratinocytes, whereas DMSO did not.

Bioluminescence

Mice were injected intraperitoneally with Xenolight RediJect Coelenterazine h (Perkin Elmer) solution and imaged using a Xenogen IVIS-200 Optical Imaging Instrument (Perkin Elmer) as described previously (6).

Tumorsphere assay

A-431 cells were cultured on growth factor-reduced Matrigel and serum-free DMEM for 72 hours to form tumorspheres (24). Tumorspheres were incubated with conditioned media (CM) from quiescent (made by a 3-day incubation in 0.2% FBS) or DOXO-induced senescent HCA2 cells. CM were generated by a 3-day incubation in 0.2% serum-media, and contained solvent, SB203580 (Selleck Chemicals) or IL1 α antibody (R&D Systems). CM were replenished every 72 hours. After 7 days, we assessed tumorsphere EdU incorporation.

Western blotting, cell proliferation assays, immunostaining, and senescence-associated β -galactosidase staining

Western blotting was performed as described previously (6, 15). Primary and secondary antibodies are listed in Supplementary Table S1. Cell proliferation was assessed using a Z1 Coulter Particle Counter (Beckman Coulter) and EdU incorporation using the Molecular Probes Click iT EdU Alexa Fluor 488 HCS Assay Kit (Thermo-Fisher Scientific) as per the manufacturer's instructions. Immunostaining was performed as described previously (15). Senescence-associated β -galactosidase (*SA- β -gal*) staining was

Alimirah et al.

assessed using the Biovision Kit (Milpitas) as per the supplier's instructions. Images were quantified from three independent fields from three biological replicates using ImageJ software and the ImageJ cell counter tool.

qRT-PCR analysis

RNA was isolated from cultured cells using the Bioline Isolate II RNA Mini Kit (Taunton). RNA was isolated from homogenized tissues using TRizol reagent (Thermo Fisher Scientific) with the Direct-zol RNA MiniPrep Kit (Genesee Scientific) as recommended by the supplier. cDNA synthesis and qRT-PCR were performed as described previously (15). Primers are listed in Supplementary Tables S2 and S3.

IHC and SA- β -gal staining of skin tissues

Human SCC and normal skin tissue arrays (SK208) were from US Biomax. Mouse skin was fixed in 10% buffered formalin (Thermo Fisher Scientific) for 7 days, transferred to 70% ethanol for 24 hours and paraffin-embedded. Tissues were cut into 7 μ m sections, deparaffinized, rehydrated, washed with PBS, and stained with hematoxylin and eosin (H&E; ref. 6). For immunostaining, tissue sections were rinsed in PBS followed by antigen retrieval using citrate buffer (Cell Signaling Technology) and the Cell Signaling Technology protocol. Skin sections were then stained overnight with antibodies from Cell Signaling Technology, listed in Supplementary Table S1, per the manufacturer's instructions.

SA- β -gal staining was performed as described previously (6). Images were obtained using an Olympus BX20 microscope; three independent fields were quantified using ImageJ software and the ImageJ cell counter tool. For vimentin quantification, three different fields were analyzed using the Color Deconvolution plug-in in ImageJ. The plugin includes a built-in vector that separates the image into three color channels. The brown channel was set to include only vimentin positive staining and then quantified for percent area.

Statistical analysis

Statistics were assessed using GraphPad Software. For time dependent tumor growth, statistical significance was determined by two-way ANOVA. Tukey test for multiple comparisons was used for all post-analyses. For *in vivo* experiments with multiple comparisons, one-way ANOVA and Sidak test for multiple comparisons were used. For pairwise comparisons, data were analyzed using the unpaired two-tailed Student *t* test. Differences between means were considered significant when values were *, $P < 0.05$ or lower; ns denotes nonsignificant. Data are presented as mean values \pm SEM or \pm SD for *in vivo* and cell culture experiments, respectively. All culture experiments were replicated at least three times.

Results

TPA induces senescence and a SASP in human keratinocytes and mouse skin

Previous studies detected senescent cells in the dermal and stromal layers of DMBA/TPA-induced papillomas and within papillomas themselves (25, 26), implicating a role for senescent cells in SCC development. Because these studies did not reveal when or how senescent cells contributed to tumor growth, we asked whether DMBA or TPA induced senescence. We treated human keratinocytes, the SCC cells of origin (22), with a single dose of increasing concentrations of DMBA (2–8 μ mol/L) or DMSO (control). The cells proliferated for 10 days after treatment, suggesting that DMBA did not induce senescence (Supplementary Fig. S1A).

To determine whether DMBA induces senescence *in vivo*, we treated dorsal skin of p16-3MR mice with a single dose of DMBA (0.25 mg/mL) or acetone (control) and analyzed whole skin and the epidermis for *p16* mRNA levels 1 month later. We followed the standard two-step skin carcinogenesis protocol of a single dose of DMBA for initiation because multiple DMBA treatments would not allow us to determine whether senescent cells act as tumor initiators or promoters. We also tested skin for SA- β -gal (27) activity and cell proliferation. A single-dose of DMBA compared with acetone yielded no differences in *p16* mRNA levels, SA- β -gal activity, or cell proliferation (assessed by immunostaining for Ki-67). Thus, a single dose of DMBA alone does not induce senescence in cultured keratinocytes or skin (Supplementary Figs. S1B–S1F).

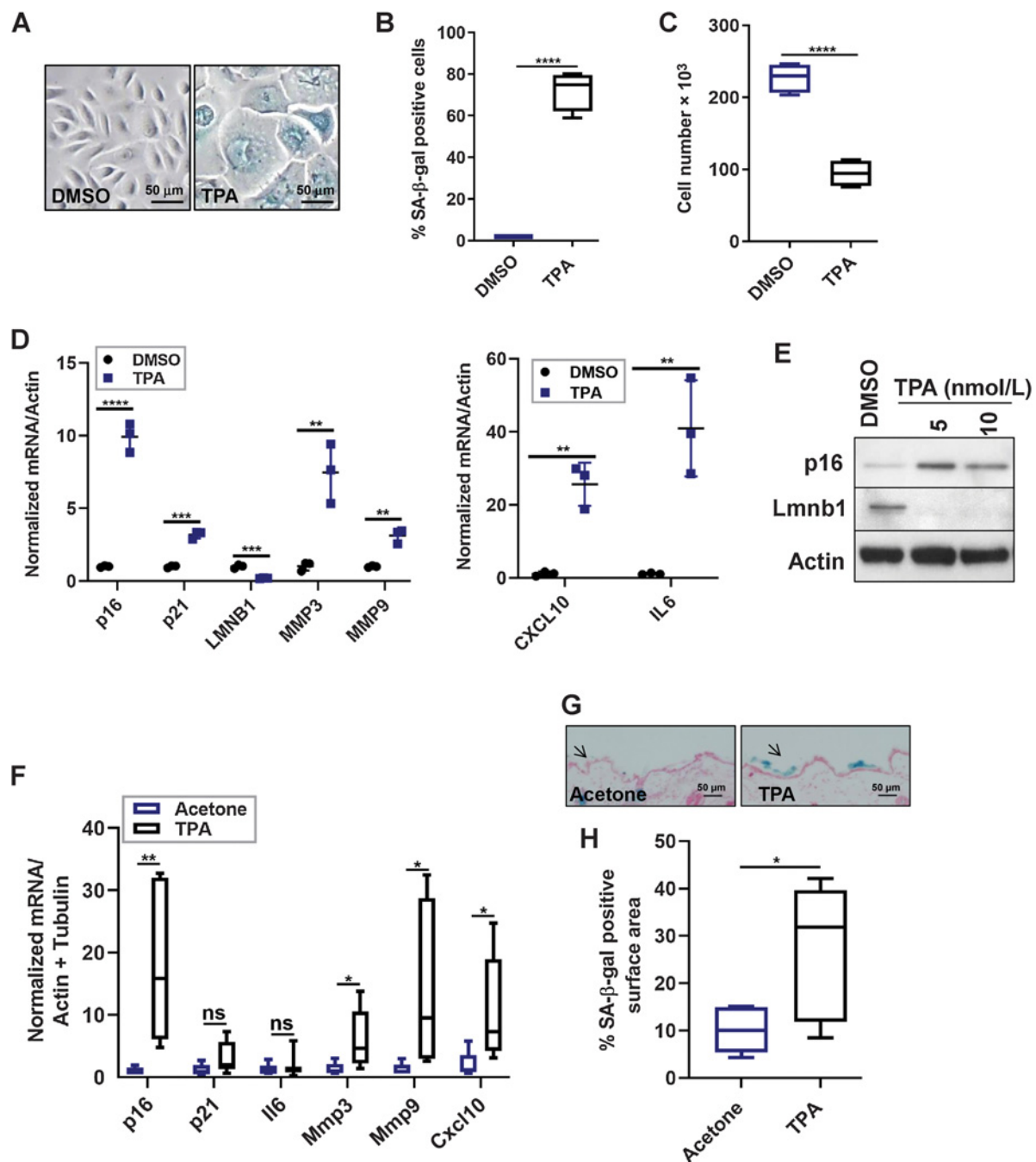
We then treated human keratinocytes with DMSO or various concentrations of TPA (1.3–10 nmol/L) and assessed senescence 12 days later. TPA inhibited cell proliferation in a dose-dependent manner, with greatest inhibition at 5 and 10 nmol/L (Supplementary Fig. S1G). TPA (10 nmol/L) also induced SA- β -gal activity (27) in >80% of cells (Fig. 1A and B), along with the inhibition of cell proliferation (Fig. 1C). Compared with DMSO-treatment, TPA reduced *Lamin B1* (*LMNB1*) mRNA levels (28) and elevated mRNA levels of the senescence markers *p16* and *p21*, and the SASP factors *IL6*, matrix metalloproteinases (*MMP*) *MMP3* and *MMP9*, and chemokine *C-X-C motif 10* (*CXCL10*) (Fig. 1D; ref. 15). Further, TPA (5 and 10 nmol/L), but not DMSO, decreased Lamin B1 (*Lmnb1*) and increased p16 protein levels (Fig. 1E).

To determine whether TPA induces senescence in skin, we topically treated dorsal skin with either acetone or TPA twice a week for 2 months. We chose a 2-month treatment because in the skin carcinogenesis protocol tumors develop 8 weeks after TPA treatment, suggesting that senescence might occur earlier. To exclude reported inflammatory effects of TPA, the skin was analyzed for senescence 1 month after the last treatment. TPA induced senescence in the skin as demonstrated by elevated levels of *p16* and SASP factor (*Mmp3*, *Mmp9*, and *Cxcl10*) mRNAs (Fig. 1F). Unlike the increased *p21* and *IL6* mRNA levels in response to TPA in human keratinocytes, there was no increase in *p21* and *Il6* mRNA levels in mouse skin, suggesting that *p21* and *Il6* are not major factors in TPA-induced senescence in this tissue (Fig. 1F). TPA-induced senescence was confirmed by the presence of SA- β -gal-positive cells in TPA-treated but not acetone-treated skin (Fig. 1G and H). These data indicate that TPA induces senescence and a SASP in human keratinocytes and mouse skin.

TPA-induced senescence (pretreatment) stimulates tumor growth

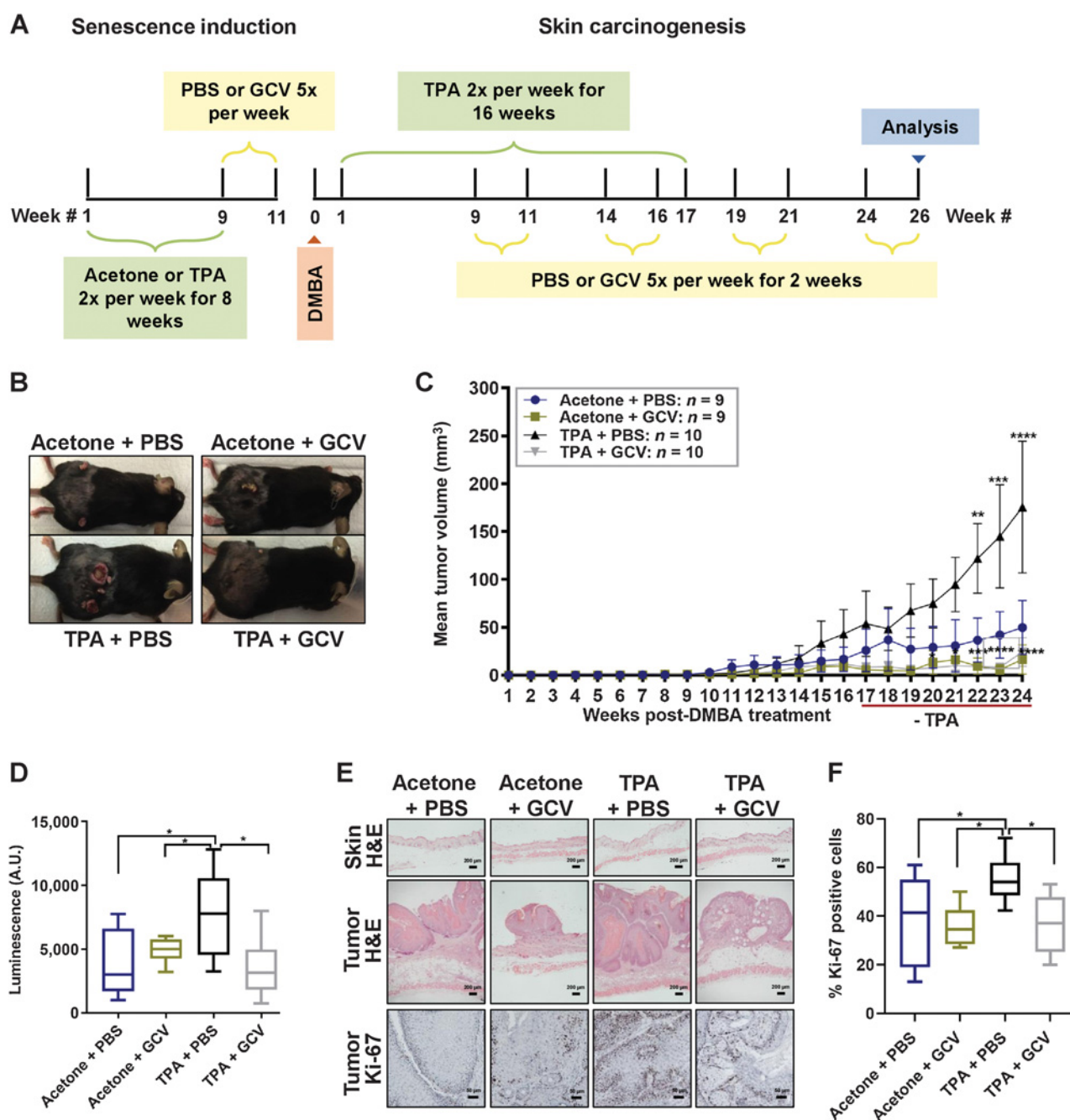
To explore the consequences of TPA-induced senescence, we asked whether TPA pretreatment facilitates tumor growth in the skin. We first induced senescence with TPA in p16-3MR mouse skin as described above. A week after the last treatment, we injected the mice with PBS or GCV to remove p16-positive senescent cells. We then implemented the two-step skin carcinogenesis protocol. To ensure the elimination of senescent cells, PBS or GCV was injected for 10 days every 3 weeks until the end of the study (Fig. 2A). Tumor growth was monitored for 24 weeks after DMBA initiation and 8 weeks after the last TPA treatment.

Starting 22 weeks after DMBA and 5 weeks after the last TPA treatment, TPA + PBS-treated mice developed significantly larger tumors than acetone + PBS, acetone + GCV, and TPA + GCV-treated mice (Fig. 2B and C). Ultimately, the mean tumor volume of TPA + PBS-treated mice was 175.5 mm³, whereas mean tumor volume of

**Figure 1.**

TPA induces senescence and a SASP in human keratinocytes and mouse skin. **A–C**, Human keratinocytes were treated with DMSO (control) or TPA (10 nmol/L) for 48 hours. Twelve days later, the cells were stained for SA- β -gal (**A** and **B**) and assessed for cell proliferation (**C**). $N = 3$ independent experiments. **D**, Total RNA was isolated from human keratinocytes and analyzed for *p16*, *p21*, and SASP mRNAs normalized to *actin*. $N = 3$ independent experiments, presented as means \pm SD. **E**, Protein lysates from human keratinocytes treated with DMSO or TPA (5 or 10 nmol/L) were evaluated for LmnB1 and p16 levels by immunoblotting. **F**, Total RNA was isolated from mouse skin topically treated with either acetone or TPA for 2 months. One month after the last treatments, the skin was analyzed for the indicated mRNAs, normalized to *actin* and *tubulin*. $N = 5$ for the acetone group; $N = 7$ for the TPA group. Shown are means \pm SEM. **G**, Frozen tissue sections of acetone- or TPA-treated skin were stained for SA- β -gal (blue) and nuclei (red). Representative images are shown (magnification, $\times 4$). Arrows, SA- β -gal positive areas. **H**, Percent of SA- β -gal positive surface area of skin compared with unstained skin. $N = 5$ for acetone group; $N = 7$ for TPA group. Shown are means \pm SEM. ns, nonsignificant; *, $P < 0.05$; **, $P < 0.01$; ***, $P < 0.001$; ****, $P < 0.0001$. (Student *t* test).

Alimirah et al.

**Figure 2.**

TPA-induced senescence (pretreatment) stimulates skin tumor growth. **A**, Schematic of treated p16-3MR mice. **B**, Representative images of tumor-bearing mice, 24 weeks after DMBA treatment. **C**, Tumors of acetone + PBS, acetone + GCV, TPA + PBS, TPA + GCV groups were monitored once a week; mean tumor volume over 24 weeks is shown. Shown are means \pm SEM. **, $P < 0.01$; ***, $P < 0.001$; ****, $P < 0.0001$ (two-way ANOVA; Tukey's test for multiple comparisons was used postanalyses). **D**, Luminescence of tumor-bearing skin in arbitrary units (A.U.) units 24 weeks after DMBA treatment. $N = 8-10$ per group. Shown are means \pm SEM. *, $P < 0.05$ (one-way ANOVA; Sidak multiple comparisons test was used postanalyses). **E**, Representative images of H&E staining of skin (top; 200 μ m) and tumors (middle; 200 μ m), and Ki-67 staining of tumors (bottom; 50 μ m). **F**, Percentage of Ki-67-positive cells in tumors from the four treatment groups. Shown are means \pm SEM. *, $P < 0.05$ (one-way ANOVA; Sidak multiple comparisons test was used postanalyses).

acetone + PBS-treated mice was 49.76 mm³. Importantly, removing senescent cells reduced tumor size in mice treated with acetone + GCV or TPA + GCV (mean volumes of 16.2 and 24.2 mm³, respectively; Fig. 2C). Notably, GCV markedly reduced tumor volume

in mice pretreated with TPA, suggesting that the senescent milieu in these mice promoted tumor growth.

To assess senescent cells in mouse skin, we used the luciferase reporter in the p16-3MR transgene (6) and measured luminescence in

mice given acetone + PBS, acetone + GCV, TPA + PBS, or TPA + GCV 24 weeks after DMBA treatment. Luminescence was significantly elevated in mice treated with TPA + PBS compared with treatment with acetone + PBS or acetone + GCV. Eliminating senescent cells decreased luminescence in TPA + GCV-treated mice, but there was no difference in luminescence between the acetone + PBS and acetone + GCV groups (Fig. 2D). Further, H&E staining of tumors and untreated skin revealed that TPA-induced senescence generates benign papillomas that were larger than tumors in mice treated with acetone + PBS, acetone + GCV, and TPA + GCV (Fig. 2E).

To determine whether the increased tumor size in TPA + PBS-treated mice was due to increased proliferation, we immunostained tumors for the proliferation marker Ki-67. The larger tumor size correlated with increased Ki-67 levels in the tumors. Importantly, eliminating senescent cells reduced Ki-67 protein levels (Fig. 2E and F). Thus, TPA promotes tumor growth in the skin by inducing senescence and eliminating senescent cells reduces tumor size.

DOXO induces senescence and a SASP in human keratinocytes and mouse skin

The long-term effects of DOXO in patients with cancer can be deleterious, often leading to secondary cancers including SCC (20, 21, 29). To understand how DOXO-induced senescence might contribute to SCC, we treated human keratinocytes with a single dose of DOXO (250 nmol/L) or DMSO (vehicle) for 24 hours and assessed senescence 10 days later. DOXO induced senescence as evidenced by SA- β -gal activity (27) in >80% of cells (Fig. 3A and B), and a significant decrease in cell proliferation (Fig. 3C). DOXO, but not vehicle, also elevated mRNA levels of *p16* and *p21* and the SASP factors *IL6*, *MMP3*, *MMP9*, and *CXCL10* (11), and decreased *LMNB1* mRNA levels (Fig. 3D; ref. 28). We confirmed elevated *p16* and reduced *LMNB1* expression at the protein levels by Western blot analyses (Fig. 3E).

To determine whether DOXO induced senescence in the skin *in vivo*, we injected p16-3MR mice with PBS or DOXO (i.p., 12 mg/kg), a dose known to induce senescence in mice (15). One month later, we assessed the presence of senescent cells. Systemic DOXO but not PBS significantly increased mRNA levels of *p16* and the SASP factors *Mmp3*, *Cxcl10* and *Il1 α* , but not *Mmp9*, *Il6*, or *p21*. Unlike TPA-induced senescence, *Mmp9* mRNA levels did not increase upon systemic DOXO treatment. Further, *p21* and *Il6* mRNA levels did not change upon DOXO treatment, consistent with our findings in TPA-treated skin (Fig. 3F). Notably, whole body luminescence increased significantly 1 month after DOXO, but not PBS, treatment, confirming widespread senescence induced by DOXO (Fig. 3G and H). Importantly, senescent cells persisted in mouse skin 1 month after DOXO exposure, creating an environment permissive for tumor growth.

DOXO-induced senescence fuels skin tumor growth

To determine whether DOXO-induced senescence drives SCC, we injected p16-3MR mice with DOXO (12 mg/kg) with a second injection (5 mg/kg) 3 days later (to ensure the persistence of senescent cells over a 6-month period), followed by the skin carcinogenesis protocol (Fig. 4A). A DOXO dose of 17 mg/kg is not toxic to these mice (15). The presence of senescent cells in DOXO-treated mice was confirmed by whole body luminescence, and by *p16* mRNA. As expected, GCV significantly reduced whole body luminescence and *p16* mRNA levels in the skin (Fig. 4B and C). Thus, DOXO-induced senescent cells were cleared prior to DMBA treatment.

Throughout the skin carcinogenesis protocol, tumor incidence (Supplementary Fig. S2A) and number (Supplementary Fig. S2B) did not significantly change across treatment groups (PBS + PBS, PBS + GCV, DOXO + PBS, and DOXO + GCV). However, 21 weeks after DMBA initiation, tumors in the DOXO-treated mice were an average size of 183 mm³ compared with 29 mm³ in the PBS-treated group. Mean tumor volumes of the PBS + GCV and DOXO + GCV-treated groups were 7.1 and 5.4 mm³, respectively, indicating that removal of senescent cells suppressed tumor growth (Fig. 4D and E). Further, 21 weeks after DMBA initiation, DOXO-injected mice weighed significantly less than PBS-treated mice, whereas GCV prevented this weight loss (Supplementary Fig. S2C). To confirm that DOXO-induced senescent cells persist independent of the skin carcinogenesis treatment regimen, skin that was not treated with DMBA/TPA from the four groups was stained for SA- β -gal activity at the end of the study. DOXO-treated mice had a higher percentage of skin area positive for SA- β -gal compared with PBS-treated mice, and this percentage declined upon elimination of senescent cells (Fig. 4F and G).

These data support the hypothesis that senescent cells can drive skin carcinogenesis, and that genotoxic drugs such as DOXO can accelerate tumor growth by inducing senescence *in vivo*.

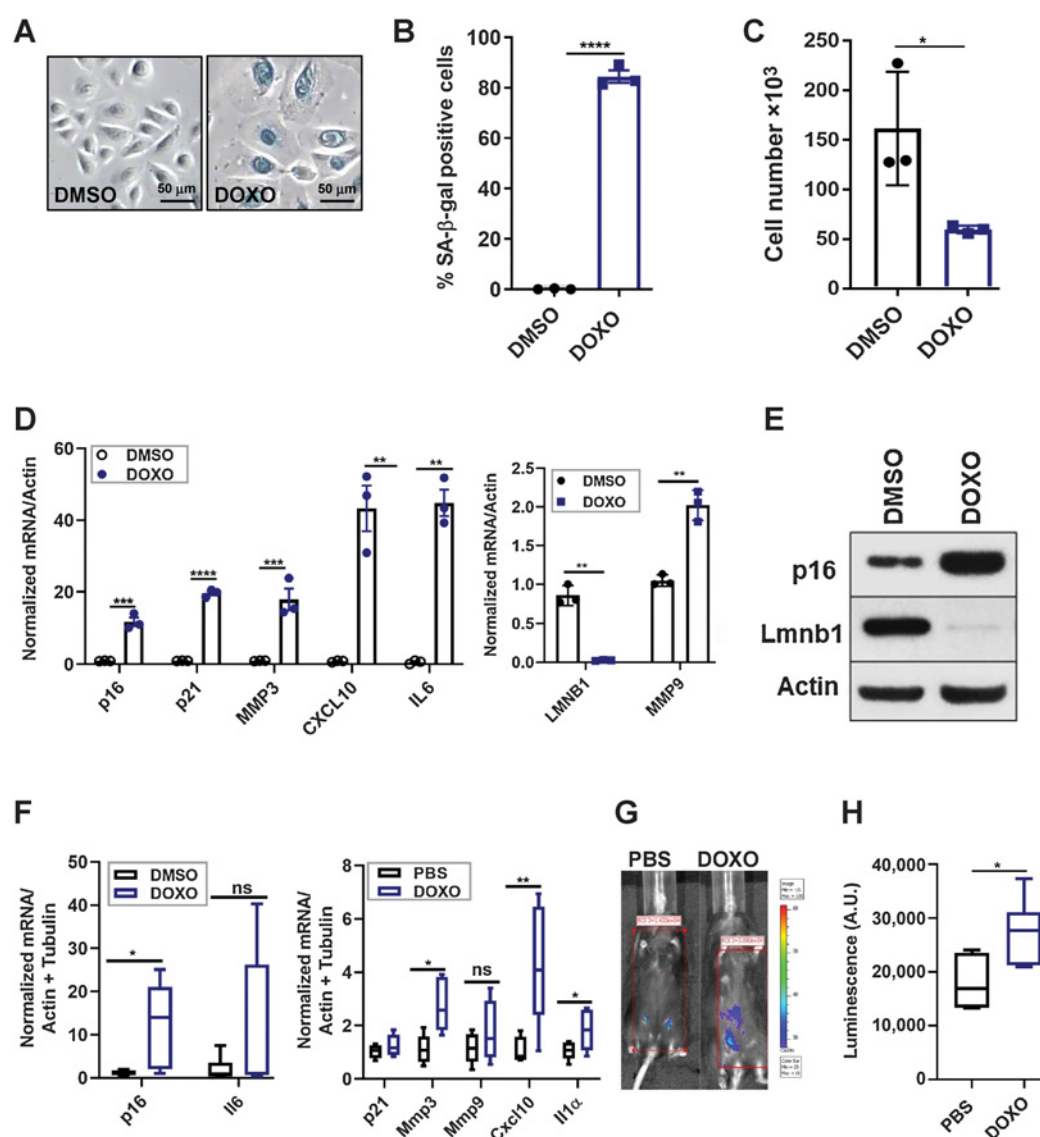
Eliminating DOXO-induced senescent cells prevents malignant progression

To identify the reason behind the increased tumor size in DOXO-versus PBS-treated mice, we characterized skin tumors from PBS + PBS, PBS + GCV, DOXO + PBS, and DOXO + GCV-treated mice. For each mouse and treatment group, we compared untreated skin (side without DMBA and TPA treatment) with DMBA- and TPA-treated skin. H&E staining revealed that ~31% (5/16) of DOXO-exposed mice developed carcinomas, whereas the other groups developed only benign papillomas (Fig. 5A). Consistent with tumor size, Ki-67 positive cells were more abundant in tumors from DOXO-treated mice compared with other treatment groups (Fig. 5B). Further, vimentin, an epithelial-mesenchymal transition marker (11, 30), was elevated at the epithelial invasive front, underlying connective tissue and the tumor itself, and vascularization was more prominent as evidenced by increased levels of CD-31-positive vessels in DOXO-compared with PBS-treated tumors. Vimentin and CD-31 levels were significantly reduced by GCV (Fig. 5C and D). Together, the results suggest that DOXO-induced senescence potentiates the conversion of benign skin papillomas to carcinomas.

The SASP drives skin carcinogenesis

The senescent fibroblast SASP is known to enhance tumor cell proliferation and invasion in culture (11, 31). Upstream SASP regulators have been identified, including p38MAPK and IL1 α (32, 33). We therefore assessed p38 phosphorylation (Thr180/Tyr182; p-p38) by Western blotting. DOXO-induced senescence elevated p38 (Thr180/Tyr182; Supplementary Fig. S3A). To determine whether this increase facilitates cancer proliferation, we used human A-431 skin carcinoma 3D-tumorspheres. We incubated the tumorspheres for 3 days in serum-free media, then incubated with CM from nonsenescent or DOXO-induced senescent HCA2 skin fibroblasts treated or not with SB203580 (SB; 10 μ mol/L), a pan p38MAPK inhibitor. Prior to treating the tumorspheres, we verified fibroblast phenotypes by SA- β -gal staining, DNA damage (γ -H2AX) foci, and *p16* mRNA levels (Supplementary Figs. S3B–S3D). Treatment of skin fibroblasts with SB reduced DOXO-induced SASP factors (Supplementary Fig. S3E). Importantly, tumorspheres exposed to CM from senescent, but not

Alimirah et al.

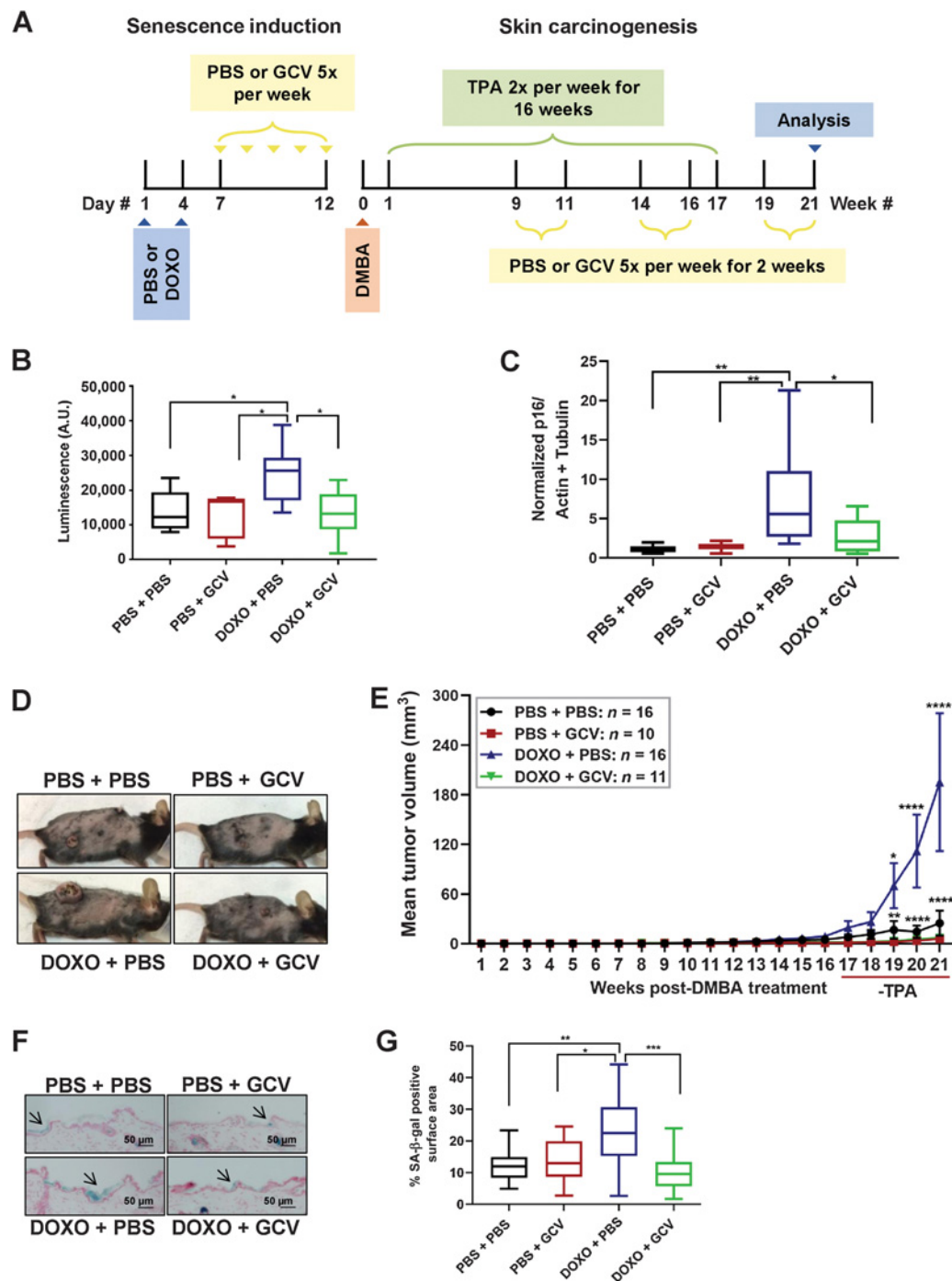
**Figure 3.**

DOXO induces senescence and a SASP in human keratinocytes and mouse skin. **A–C**, Human keratinocytes were treated with DMSO or DOXO (250 nmol/L) for 24 hours. Ten days later, the cells were stained for SA-β-gal (**A** and **B**) and assessed for cell proliferation (**C**). $N = 3$ independent experiments. Shown are means \pm SD. **D**, Total RNA was isolated from the indicated cells and analyzed for *p16*, *p21*, and SASP mRNAs, normalized to *actin*. $N = 3$ independent experiments. Shown are means \pm SD. **E**, Protein lysates from human keratinocytes were evaluated for p16 and LMNB1 by immunoblotting. **F**, Total RNA was isolated from the skin of PBS- or DOXO-treated mice and analyzed for the indicated mRNAs, normalized to *actin* and *tubulin*. $N = 6$ per each treatment group. Shown are means \pm SEM. **G** and **H**, Representative image (**G**) and quantification (**H**) in arbitrary units (A.U.) of whole-body luminescence of p16-3MR mice 1 month after PBS or DOXO treatments. $N = 6$ per each treatment group. Shown are means \pm SEM. ns, nonsignificant; *, $P < 0.05$; **, $P < 0.01$; ***, $P < 0.001$; ****, $P < 0.0001$. (Student *t* test).

nonsenescent, fibroblasts incorporated more EdU, indicative of increased proliferation, which was reduced by p38MAPK inhibition (**Fig. 6A** and **B**). Because *IL1α* mRNA expression also increased in mouse skin in response to DOXO, we inhibited *IL1α* signaling in DOXO-treated skin fibroblasts using an *IL1α* neutralizing antibody; the antibody reduced the DOXO-induced SASP (Supplementary Fig. S3F). *IL1α* inhibition also reduced tumorsphere proliferation (EdU incorporation; **Fig. 6C** and **D**). These findings show that DOXO-induced senescence promotes SCC progression by elevating

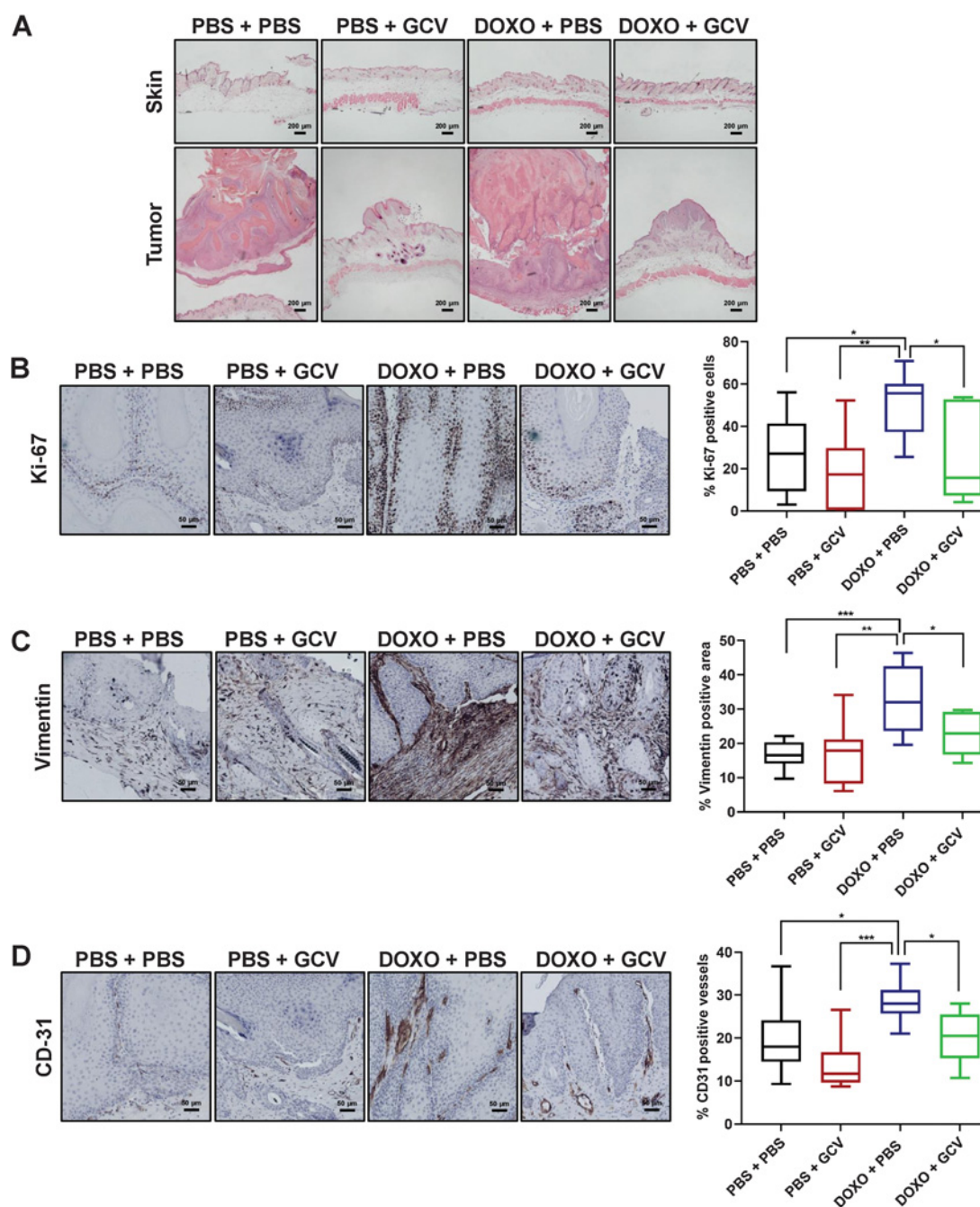
p38MAPK and *IL1α* signaling, two upstream mediators of the SASP, in the skin microenvironment.

To test these findings in mice, we asked whether senescence and SASP markers were present in skin adjacent to tumors and/or within the tumors themselves. Senescent cells adjacent to tumors would indicate that senescence in the microenvironment can fuel cancer growth, whereas senescent cells within tumors would suggest that tumor-associated senescence can exacerbate tumor growth.

**Figure 4.**

DOXO-induced senescence fuels skin tumor growth. **A**, A schematic of the PBS/DOXO and skin carcinogenesis regimens of p16-3MR mice. TPA treatment lasted 16 weeks. **B**, Quantification of whole-body luminescence of p16-3MR mice 10 days after PBS/DOXO treatments and 1 week after DMBA initiation. Quantification is in arbitrary units (A.U.). Shown are means \pm SEM. *, $P < 0.05$ (one-way ANOVA; Sidak multiple comparisons test was used postanalyses). **C**, Total RNA was isolated from the skin of the four treatment groups and analyzed for *p16* normalized to *actin* and *tubulin* (PBS + PBS, $n = 10$; PBS + GCV, $n = 8$; DOXO + PBS, $n = 9$; DOXO + GCV, $n = 8$). Shown are means \pm SEM. *, $P < 0.05$; **, $P < 0.01$ (one-way ANOVA; Sidak multiple comparisons test was used postanalyses). **D**, Representative images of tumor-bearing mice 21 weeks after DMBA treatment and 5 weeks after TPA treatment in PBS + PBS, PBS + GCV, DOXO + PBS, DOXO + GCV groups. **E**, The mean tumor volume of the same mice is shown over 21 weeks. Shown are means \pm SEM. *, $P < 0.05$; **, $P < 0.01$; ****, $P < 0.0001$ (two-way ANOVA; Tukey test for multiple comparisons was used postanalyses). **F**, Frozen skin sections of treatment groups (PBS + PBS, $n = 10$; PBS + GCV, $n = 10$; DOXO + PBS, $n = 14$; DOXO + GCV, $n = 14$) were stained for SA- β -gal (blue) and nuclei (red). Representative images are shown (50 μ m). Arrows, SA- β -gal positive areas. **G**, Percent of SA- β -gal positive surface area of skin compared with nonstained skin. Shown are means \pm SEM. *, $P < 0.05$; **, $P < 0.01$; ***, $P < 0.001$ (one-way ANOVA; Sidak multiple comparisons test was used postanalyses).

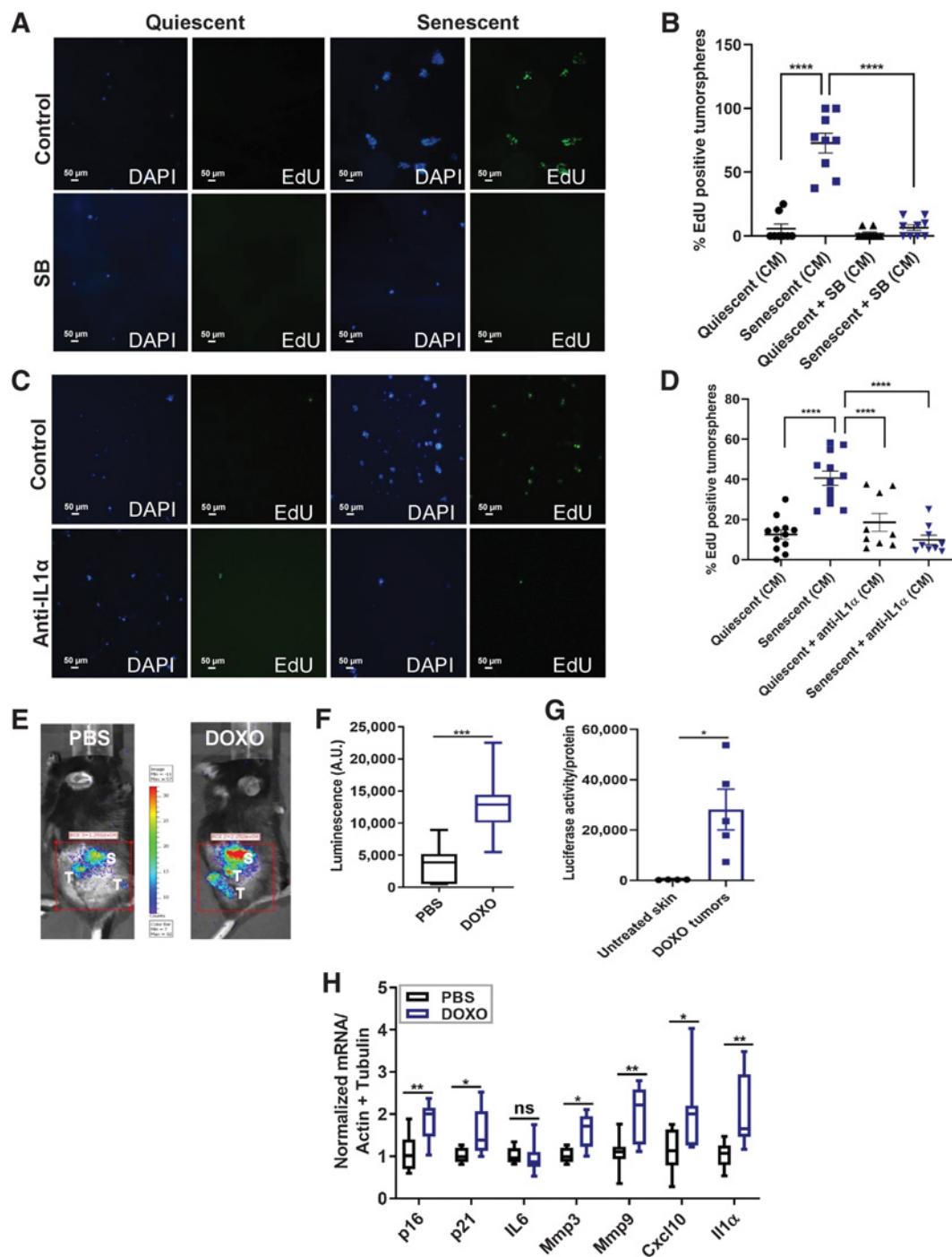
Alimirah et al.

**Figure 5.**

Eliminating DOXO-induced senescent cells prevents malignant tumor development. **A**, Representative images of H&E staining of the skin (top) and tumors (bottom) in PBS + PBS, PBS + GCV, DOXO + PBS, DOXO + GCV-treated groups (200 μ m). **B–D**, In the same four groups (PBS + PBS, $n = 9$; PBS + GCV, $n = 7$; DOXO + PBS, $n = 11$; DOXO + GCV, $n = 7$), representative IHC images for Ki-67 (**B**), vimentin (**C**), and CD-31 (**D**; 50 μ m) with the corresponding quantification of percent positive cells in the right panels. Shown are means \pm SEM. *, $P < 0.05$; **, $P < 0.01$; ***, $P < 0.001$ (one-way ANOVA; Sidak multiple comparisons test was used postanalyses).

To verify the chronic presence of senescent cells throughout the body months after DOXO treatment, we assessed whole body luminescence in PBS- or DOXO-treated mice 21 weeks after DMBA initiation and 5 weeks after TPA removal. Luminescence was higher in DOXO-treated, compared with PBS-treated, mice, suggesting that senescent cells persist weeks after DOXO exposure (Supplementary

Figs. S3G and S3H). To evaluate senescent cells adjacent to tumors, we imaged DMBA/TPA-treated skin of PBS or DOXO-injected mice 21 weeks after DMBA treatment. Luminescence was apparent in skin adjacent to and within tumors (Fig. 6E and F). Further, DOXO-injected mice had significantly higher luminescence compared with PBS-treated mice (Fig. 6E and F), and luminescence was higher in

**Figure 6.**

The SASP drives skin carcinogenesis. **A–D**, Representative images and quantification of tumorspheres of A-431 cells embedded in reduced growth factor Matrigel incubated for 7 days with CM from nonsenescent (quiescent) or senescent HCA2 fibroblasts with or without SB203580 (**A** and **B**) or anti-IL1 α (**C** and **D**). **A** and **C**, Tumorspheres are shown stained with DAPI (blue) and EdU (green). **B** and **D**, Quantification of percentage EdU-positive cells. $N = 3$ independent experiments. Shown are mean \pm SEM. **, $P < 0.01$; ****, $P < 0.0001$ (one-way ANOVA; Sidak multiple comparisons test was used postanalyses). **E**, Representative tumor and adjacent skin luminescence images of PBS- or DOXO-treated mice, 21 weeks after DMBA treatment and 5 weeks after the last TPA treatment. Luminescent skin and tumors are labeled on the images as S and T, respectively. **F**, Luminescence quantification of tumors and adjacent skin shown in **E** in arbitrary units (A.U.). $N = 8$ per each treatment group. Shown are mean \pm SEM. ***, $P < 0.001$ (Student t test). **G**, Luciferase activity of untreated skin compared with DOXO-tumor; protein lysates were normalized to total protein content. $N = 4$ –5 for skin and DOXO tumors, respectively. Shown are mean \pm SEM. *, $P < 0.05$ (Student t test). **H**, Total RNA was isolated from skin adjacent to tumors from mice in **E** and **F** and analyzed for the indicated mRNAs, normalized to *actin* and *tubulin*. $N = 8$ per treatment group. Shown are mean \pm SEM. ns, nonsignificant; *, $P < 0.05$; **, $P < 0.001$ (Student t test).

DOXO-treated tumors compared with untreated skin, indicating the presence of senescent cells within the tumors (Fig. 6G). Moreover, mRNA levels of *p16*, *p21*, and the SASP factors *Mmp9*, *Mmp3*, *Cxcl10* and *Il1 α* were higher in skin adjacent to tumors in DOXO-treated compared with PBS-treated mice (Fig. 6H). This elevation was accompanied by increased mRNA levels of the skin stem cell genes *Cd34*, *Lgr6*, and *Lrig1* (Supplementary Fig. S3I; ref. 26). These findings suggest that DOXO-induced senescence and the SASP promote skin carcinogenesis by enhancing stemness in the skin microenvironment.

A subset of macrophages was reported to express p16 and SA- β -gal in mouse tissues (34), and neutrophils, important orchestrators of inflammation, secrete proinflammatory molecules similar to the SASP (35). Thus, neutrophils and macrophages might contribute to the microenvironment that promotes cancer development (35, 36). To test the possibility that macrophages and/or neutrophils, not senescent cells, drive SCC, we assessed mRNA levels of the macrophage marker *Cd68* (37) and neutrophil markers *elastase* (*Ela*; ref. 38) and *myeloperoxidase* (*Mpo*; ref. 39) in the skin of PBS- or DOXO-treated mice. There were no differences in these markers between the two groups (Supplementary Fig. S4A). To confirm these findings, we stained tissue sections from PBS- and DOXO-treated mice for the macrophage marker F4/80 (37) and the neutrophil marker Ly6G (40). Consistent with the mRNA data, we observed no difference in the levels of F4/80 and Ly6G in PBS- and DOXO-treated mice (Supplementary Figs. S4B and S4C). These findings suggest that DOXO induces senescence and a SASP in the skin, independent of macrophages and neutrophils.

To confirm that senescent cells were present within skin tumors, we compared luciferase activity in untreated skin and DOXO-induced tumors in p16-3MR mice. Luminescence was evident only in tumors, not in untreated skin, further indicating that p16-positive senescent cells are present in the tumors (Fig. 6G). Together, these findings suggest that DOXO-induced senescence and the SASP occur throughout the body, but also both in skin adjacent to tumors and within tumors. Additionally, they suggest that the SASP within tumors may facilitate tumor growth in addition to the SASP in the skin microenvironment. Thus, senescent cells in tumors might reinforce tumor growth fueled by the senescent microenvironment.

p38MAPK and p44/42 ERK/MAPK signaling increase in tumors from DOXO-treated mice

p38MAPK and ERK/MAPK(p44/42) signaling are known to promote the SASP and tumor progression, respectively (32, 41). The expression of p-p38 (Thr180/Tyr182) MAPK in skin tumors *in vivo* was elevated in DOXO-treated, compared with PBS-treated, mice. Moreover, this elevation declined upon removing senescent cells with GCV (Fig. 7A). Likewise, p-p44/42MAPK increased in tumors from DOXO-treated compared with PBS-treated mice and this increase declined upon elimination of senescent cells (Fig. 7B).

To determine the translational significance of p38 and p44/42MAPK activation, we compared protein expression of p-p38 (Thr180/Tyr182) and p-p44/42 in commercially available human (h) SCC and normal skin tissue arrays. p38 and p44/42MAPK phosphorylation was elevated in 77% of hSCC lesions (grades I–III) compared with normal skin, supporting our finding that these pathways might contribute to malignancy after induction of senescence (Fig. 7C and D). Thus, DOXO-induced senescence and the SASP might contribute to p38 and p44/42MAPK signaling within skin tumors and in the microenvironment surrounding the tumors, reinforcing tumor growth by increasing stemness and converting benign papillomas to carcinomas (Fig. 7E).

Discussion

SCC incidence rises after genotoxic cancer treatments (20, 21). The mechanism behind this increase, decades after chemotherapy, remains elusive. Using two senescence inducers (TPA and DOXO) and p16-3MR mice, we show that cellular senescence drives skin carcinogenesis. TPA is an established tumor promoter that can stimulate cell proliferation (22). We show that TPA also promotes carcinogenesis by inducing p16-dependent senescence, accompanied by a SASP. Strikingly, removal of TPA-induced senescent cells in p16-3MR mice reduced tumor growth. Acute TPA treatment can also lead to the secretion of inflammatory chemokines, cytokines, proteases, and growth factors that stimulate tumor growth, analogous to the SASP. However, these effects of TPA can be reversed, depending on the number of applications and treatment duration (42). We show that once TPA is removed, tumor growth accelerates, suggesting that senescent cells, not the inflammation caused by TPA, drive tumor growth.

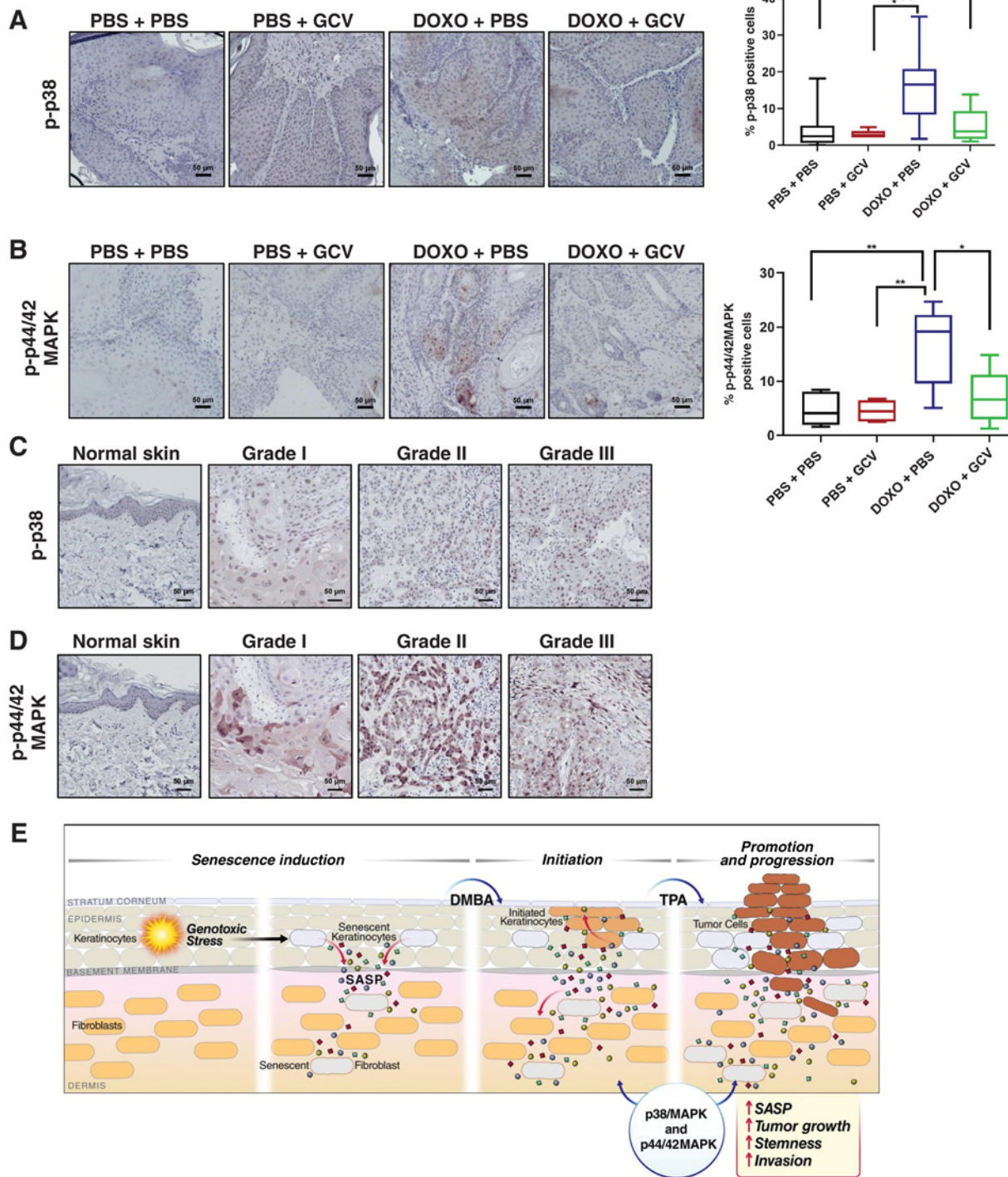
Chemotherapeutic agents, such as DOXO, induce cellular senescence and a SASP (15). Therefore, chemotherapy-induced senescence might contribute to SCC development. Indeed, treating mice with DOXO resulted in a persistent senescent microenvironment in the skin, which was conducive to tumor growth. After DOXO and DMBA/TPA treatments, senescent cells were present throughout the body, including the skin adjacent to tumors and within the tumors. Thus, not only are DOXO-induced senescent cells present throughout the body, they are also present adjacent to and within the tumors, exacerbating tumor growth. Because DOXO was administered systemically, it is difficult to discern to what extent senescent cells in organs other than skin, or SASP factors in the circulation, contribute to skin cancer growth. For example, we previously showed that DOXO induces senescence and a SASP in the liver, concomitant with an elevation in the SASP factors *Il6* and *Cxcl1* in sera (15). It is therefore plausible that senescent cells throughout the body might also contribute to skin tumor progression.

One deleterious side effect of chemotherapy in patients with cancer is weight loss (43). We show here that removal of senescent cells periodically for 21 weeks prevents the weight loss caused by DOXO. Thus, removing senescent cells might improve cancer patients' overall well-being.

The senescence fueled skin tumor growth in our study is primarily p16-dependent. TPA and DOXO treatments alone elevated *p16*, but not *p21*, mRNA levels 1 month after treatment. However, DOXO, DMBA, and TPA treatments together increased *p21* mRNA in skin adjacent to tumors. These data suggest that a higher senescence burden, or different quality of senescent cells, might occur later during skin carcinogenesis. In addition, not all SASP factors increased in the skin after DOXO or TPA treatment alone. For instance, TPA-induced senescence elevated expression of the SASP factors *Mmp3*, *Mmp9*, and *Cxcl10*, whereas DOXO-induced senescence elevated *Mmp3*, *Il1 α* , and *Cxcl10*, but not *Mmp9*, mRNA levels.

Cxcl10, which acts through its receptor CXCR3, is highly expressed in several cancers (44), and is associated with metastasis and poor survival (45). MMPs degrade the extracellular matrix and elevated levels of MMPs often mark aggressive forms of cancer (46, 47). For example, elevated MMP9 in stromal cells of the skin enhances SCC development (47), and *Il1 α* promotes the growth of several cancers (48). Collectively, these studies support our data that the SASP, including *Cxcl10* and MMPs, might promote senescence-induced skin carcinogenesis.

Senescence and Skin Carcinogenesis

**Figure 7.**

Phospho-p38 and phospho-p44/42MAPK signaling is increased in tumors from DOXO-treated mice. **A** and **B**, Representative IHC images of tumors from PBS + PBS ($n = 9$), PBS + GCV ($n = 7$), DOXO + PBS ($n = 11$), DOXO + GCV ($n = 7$), stained with p-p38 (**A**) or p-p44/42 (**B**), with the corresponding quantification of percent positive cells in the right panels. Shown are means \pm SEM. *, $P < 0.05$; **, $P < 0.01$; one-way ANOVA; Sidak multiple comparisons test was used postanalyses. **C** and **D**, Representative IHC images of normal human skin and hSCC lesions (grades I-III) stained with p-p38 (**C**) and p-p44/42 (**D**). **E**, Working model showing that DOXO induces senescence and a SASP in keratinocytes and fibroblasts, creating a microenvironment permissible for tumor growth and invasion. Once tumors are formed, senescent cells within the tumors also reinforce tumor growth by elevating p-p38 and p-p44/42 signaling.

Alimirah et al.

The chronic presence of senescent cells has been linked to tumor cell proliferation. For example, we showed that senescent fibroblasts promote premalignant epithelial cell growth in culture, and caused premalignant cells to form tumors in immune-compromised mice (49). In addition, our recent study revealed that DOXO treatment enhanced lung metastases of Polyoma Virus middle T antigen-expressing breast cancer cells transplanted into the mammary fat pad, and that systemic elimination of senescent cells reduced these metastases (15). Although these studies show an association between senescent cells and carcinogenesis, they used exogenously administered cancer cell lines *in vivo*. In our study, we monitored skin tumor growth throughout the initiation, promotion, and progression stages of endogenous tumor development. Thus, our study more closely recapitulates human tumor pathogenesis, identifying senescence as a potential culprit behind tumor promotion and the conversion of benign papillomas to carcinomas.

Cancer recurrence and the development of second neoplasms in cancer survivors, decades after chemotherapy, is an emerging public health concern (17, 50). Chemotherapy-induced senescence might contribute to cancer recurrence and second cancer development. Our study suggests a direct link between the presence of DOXO-induced senescent cells and tumor promotion in a model of SCC. Our findings may help develop senolytics aimed at eliminating senescence-fueled skin cancer.

Disclosure of Potential Conflicts of Interest

J. Campisi reports grants from Unity Biotechnology during the conduct of the study and is a founder of Unity Biotechnology, and with M. Demaria owns shares in

the company outside the submitted work. No potential conflicts of interest were disclosed by the other authors.

Authors' Contributions

F. Alimirah: Conceptualization, formal analysis, supervision, funding acquisition, validation, investigation, visualization, writing-original draft, writing-review and editing. **T. Pulido:** Formal analysis, validation, investigation, visualization. **A. Valdovinos:** Formal analysis, validation and investigation. **S. Alptekin:** Formal analysis, validation and investigation. **E. Chang:** Formal analysis, validation and investigation. **E. Jones:** Formal analysis, validation and investigation. **D.A. Diaz:** Investigation. **J. Flores:** Investigation. **M.C. Velarde:** Investigation. **M. Demaria:** Investigation. **A. R. Davalos:** Investigation. **C.D. Wiley:** Investigation. **C. Limbad:** Investigation. **P.-Y. Desprez:** Formal analysis, investigation, writing-review and editing. **J. Campisi:** Conceptualization, resources, formal analysis, supervision, funding acquisition, validation, methodology, writing-review and editing.

Acknowledgments

This work was supported by NIH grants F32 AG044946 to F. Alimirah and AG09909 and AG017242 to J. Campisi, and funds from the Hillblom Foundation. We thank Dr. Aseem Lal for histological analysis of the skin and tumors.

The costs of publication of this article were defrayed in part by the payment of page charges. This article must therefore be hereby marked *advertisement* in accordance with 18 U.S.C. Section 1734 solely to indicate this fact.

Received January 13, 2020; revised May 9, 2020; accepted June 29, 2020; published first July 8, 2020.

References

- Rodier F, Campisi J. Four faces of cellular senescence. *J Cell Biol* 2011;192:547–56.
- Wiley CD, Velarde MC, Lecot P, Liu S, Sarnoski EA, Freund A, et al. Mitochondrial dysfunction induces senescence with a distinct secretory phenotype. *Cell Metab* 2016;23:303–14.
- Harley CB, Futcher AB, Greider CW. Telomeres shorten during aging of human fibroblasts. *Nature* 1990;345:458–60.
- Serrano M, Lin AW, McCurrach ME, Beach D, Lowe SW. Oncogenic ras provokes premature cell senescence associated with accumulation of p53 and p16INK4a. *Cell* 1997;88:593–602.
- Zhang R, Adams PD. Heterochromatin and its relationship to cell senescence and cancer therapy. *Cell Cycle* 2007;6:784–9.
- Demaria M, Ohtani N, Youssef SA, Rodier F, Toussaint W, Mitchell JR, et al. An essential role for senescent cells in optimal wound healing through secretion of PDGF-AA. *Dev Cell* 2014;31:722–33.
- Mosteiro L, Pantoja C, Alcazar N, Marion RM, Chondronasiou D, Rovira M, et al. Tissue damage and senescence provide critical signals for cellular reprogramming *in vivo*. *Science* 2016;354:aaf4445.
- Storer M, Mas A, Robert-Moreno A, Pecoraro M, Ortells MC, Di Giacomo V, et al. Senescence is a developmental mechanism that contributes to embryonic growth and patterning. *Cell* 2013;155:1119–30.
- Munoz-Espin D, Canamero M, Maraver A, Gomez-Lopez G, Contreras J, Murillo-Cuesta S, et al. Programmed cell senescence during mammalian embryonic development. *Cell* 2013;155:1104–18.
- Lecot P, Alimirah F, Desprez PY, Campisi J, Wiley C. Context-dependent effects of cellular senescence in cancer development. *Br J Cancer* 2016;114:1180–4.
- Coppe JP, Patil CK, Rodier F, Sun Y, Munoz DP, Goldstein J, et al. Senescence-associated secretory phenotypes reveal cell-nonautonomous functions of oncogenic RAS and the p53 tumor suppressor. *PLoS Biol* 2008;6:2853–68.
- Baker DJ, Childs BG, Durik M, Wijers ME, Sieben CJ, Zhong J, et al. Naturally occurring p16(Ink4a)-positive cells shorten healthy lifespan. *Nature* 2016;530:184–9.
- Bussian TJ, Aziz A, Meyer CF, Swenson BL, van Deursen JM, Baker DJ. Clearance of senescent glial cells prevents tau-dependent pathology and cognitive decline. *Nature* 2018;562:578–82.
- Schafer MJ, White TA, Iijima K, Haak AJ, Ligresti G, Atkinson EJ, et al. Cellular senescence mediates fibrotic pulmonary disease. *Nat Commun* 2017;8:14532.
- Demaria M, O'Leary MN, Chang J, Shao L, Liu S, Alimirah F, et al. Cellular senescence promotes adverse effects of chemotherapy and cancer relapse. *Cancer Discov* 2017;7:165–76.
- Laberge RM, Adler D, DeMaria M, Mechtouf N, Teachenor R, Cardin GB, et al. Mitochondrial DNA damage induces apoptosis in senescent cells. *Cell Death Dis* 2013;4:e727.
- Turcotte LM, Neglia JP, Reulen RC, Ronckers CM, van Leeuwen FE, Morton LM, et al. Risk, risk factors, and surveillance of subsequent malignant neoplasms in survivors of childhood Cancer: A Review. *J Clin Oncol* 2018;36:2145–52.
- Le ON, Rodier F, Fontaine F, Coppe JP, Campisi J, DeGregori J, et al. Ionizing radiation-induced long-term expression of senescence markers in mice is independent of p53 and immune status. *Aging Cell* 2010;9:398–409.
- Que SKT, Zwald FO, Schmults CD. Cutaneous squamous cell carcinoma: Incidence, risk factors, diagnosis, and staging. *J Am Acad Dermatol* 2018;78:237–47.
- Pezzoli M, Bona Galvagno M, Bongioanni G. Oral squamous cell carcinoma in a patient treated with long-term pegylated liposomal doxorubicin for recurrent ovarian cancer. *BMJ Case Rep* 2015;2015:bcr2014204056.
- Lauvin R, Miglianico L, Hellegouarc'h R. Skin cancer occurring 10 years after the extravasation of doxorubicin. *N Engl J Med* 1995;332:754.
- Abel EL, Angel JM, Kiguchi K, DiGiovanni J. Multi-stage chemical carcinogenesis in mouse skin: fundamentals and applications. *Nat Protoc* 2009;4:1350–62.
- Beausejour CM, Krtolica A, Galimi F, Narita M, Lowe SW, Yaswen P, et al. Reversal of human cellular senescence: roles of the p53 and p16 pathways. *EMBO J* 2003;22:4212–22.
- Shaw FL, Harrison H, Spence K, Ablett MP, Simoes BM, Farnie G, et al. A detailed mammosphere assay protocol for the quantification of breast stem cell activity. *J Mammary Gland Biol Neoplasia* 2012;17:111–7.
- Collado M, Gil J, Efeyan A, Guerra C, Schuhmacher AJ, Barradas M, et al. Tumour biology: senescence in premalignant tumours. *Nature* 2005;436:642.
- Ritschka B, Storer M, Mas A, Heinzmann F, Ortells MC, Morton JP, et al. The senescence-associated secretory phenotype induces cellular plasticity and tissue regeneration. *Genes Dev* 2017;31:172–83.

27. Dimri GP, Lee X, Basile G, Acosta M, Scott G, Roskelley C, et al. A biomarker that identifies senescent human cells in culture and in aging skin in vivo. *Proc Natl Acad Sci U S A* 1995;92:9363–7.
28. Freund A, Laberge RM, Demaria M, Campisi J. Lamin B1 loss is a senescence-associated biomarker. *Mol Biol Cell* 2012;23:2066–75.
29. Cannon TL, Lai DW, Hirsch D, Delacure M, Downey A, Kerr AR, et al. Squamous cell carcinoma of the oral cavity in nonsmoking women: a new and unusual complication of chemotherapy for recurrent ovarian cancer. *Oncologist* 2012;17:1541–6.
30. Satelli A, Li S. Vimentin in cancer and its potential as a molecular target for cancer therapy. *Cell Mol Life Sci* 2011;68:3033–46.
31. Rodier F, Coppe JP, Patil CK, Hoeijmakers WA, Munoz DP, Raza SR, et al. Persistent DNA damage signalling triggers senescence-associated inflammatory cytokine secretion. *Nat Cell Biol* 2009;11:973–9.
32. Freund A, Patil CK, Campisi J. p38MAPK is a novel DNA damage response-independent regulator of the senescence-associated secretory phenotype. *EMBO J* 2011;30:1536–48.
33. Orjalo AV, Bhaumik D, Gengler BK, Scott GK, Campisi J. Cell surface-bound IL-1alpha is an upstream regulator of the senescence-associated IL-6/IL-8 cytokine network. *Proc Natl Acad Sci U S A* 2009;106:17031–6.
34. Hall BM, Balan V, Gleiberman AS, Strom E, Krasnov P, Virtuoso LP, et al. Aging of mice is associated with p16(Ink4a)- and beta-galactosidase-positive macrophage accumulation that can be induced in young mice by senescent cells. *Aging* 2016;8:1294–315.
35. Rosales C. Neutrophil: A Cell with Many Roles in Inflammation or Several Cell Types. *Front Physiol* 2018;9:113.
36. Jackaman C, Tomay F, Duong L, Abdol Razak NB, Pixley FJ, Metharom P, et al. Aging and cancer: the role of macrophages and neutrophils. *Ageing Res Rev* 2017;36:105–16.
37. Xu M, Pirtskhalava T, Farr JN, Weigand BM, Palmer AK, Weivoda MM, et al. Senolytics improve physical function and increase lifespan in old age. *Nat Med* 2018;24:1246–56.
38. Lammers AM, van de Kerkhof PC, Schalwijk J, Mier PD. Elastase, a marker for neutrophils in skin infiltrates. *Br J Dermatol* 1986;115:181–6.
39. Lau D, Mollnau H, Eiserich JP, Freeman BA, Daiber A, Gehling UM, et al. Myeloperoxidase mediates neutrophil activation by association with CD11b/CD18 integrins. *Proc Natl Acad Sci U S A* 2005;102:431–6.
40. John DS, Aschenbach J, Kruger B, Sandler M, Weiss FU, Mayerle J, et al. Deficiency of cathepsin C ameliorates severity of acute pancreatitis by reduction of neutrophil elastase activation and cleavage of E-cadherin. *J Biol Chem* 2019;294:697–707.
41. Sullivan RJ, Infante JR, Janku F, Wong DJL, Sosman JA, Keedy V, et al. First-in-class ERK1/2 inhibitor ulixertinib (BVD-523) in patients with MAPK mutant advanced solid tumors: results of a phase I dose-escalation and expansion study. *Cancer Discov* 2018;8:184–95.
42. Rundhaug JE, Fischer SM. Molecular mechanisms of mouse skin tumor promotion. *Cancers* 2010;2:436–82.
43. Takayoshi K, Uchino K, Nakano M, Ikejiri K, Baba E. Weight loss during initial chemotherapy predicts survival in patients with advanced gastric cancer. *Nutr Cancer* 2017;69:408–15.
44. Liu M, Guo S, Stiles JK. The emerging role of CXCL10 in cancer (Review). *Oncol Lett* 2011;2:583–9.
45. Wightman SC, Uppal A, Pitroda SP, Ganai S, Burnette B, Stack M, et al. Oncogenic CXCL10 signalling drives metastasis development and poor clinical outcome. *Br J Cancer* 2015;113:327–35.
46. Kerkela E, Saarialho-Kere U. Matrix metalloproteinases in tumor progression: focus on basal and squamous cell skin cancer. *Exp Dermatol* 2003;12:109–25.
47. Coussens LM, Tinkle CL, Hanahan D, Werb Z. MMP-9 supplied by bone marrow-derived cells contributes to skin carcinogenesis. *Cell* 2000;103:481–90.
48. Lewis AM, Varghese S, Xu H, Alexander HR. Interleukin-1 and cancer progression: the emerging role of interleukin-1 receptor antagonist as a novel therapeutic agent in cancer treatment. *J Transl Med* 2006;4:48.
49. Krtolica A, Parrinello S, Lockett S, Desprez PY, Campisi J. Senescent fibroblasts promote epithelial cell growth and tumorigenesis: a link between cancer and aging. *Proc Natl Acad Sci U S A* 2001;98:12072–7.
50. Guida JL, Ahles TA, Belsky D, Campisi J, Cohen HJ, DeGregori J, et al. Measuring aging and identifying aging phenotypes in cancer survivors. *J Natl Cancer Inst* 2019;111:1245–54.

Cancer Research

The Journal of Cancer Research (1916–1930) | The American Journal of Cancer (1931–1940)

Cellular Senescence Promotes Skin Carcinogenesis through p38MAPK and p44/42MAPK Signaling

Fatouma Alimirah, Tanya Pulido, Alexis Valdovinos, et al.

Cancer Res 2020;80:3606-3619. Published OnlineFirst July 8, 2020.**Updated version** Access the most recent version of this article at:
doi:[10.1158/0008-5472.CAN-20-0108](https://doi.org/10.1158/0008-5472.CAN-20-0108)**Supplementary Material** Access the most recent supplemental material at:
<http://cancerres.aacrjournals.org/content/suppl/2020/07/07/0008-5472.CAN-20-0108.DC1>**Visual Overview** A diagrammatic summary of the major findings and biological implications:
<http://cancerres.aacrjournals.org/content/80/17/3606/F1.large.jpg>**Cited articles** This article cites 50 articles, 15 of which you can access for free at:
<http://cancerres.aacrjournals.org/content/80/17/3606.full#ref-list-1>**E-mail alerts** [Sign up to receive free email-alerts](#) related to this article or journal.**Reprints and Subscriptions** To order reprints of this article or to subscribe to the journal, contact the AACR Publications Department at pubs@aacr.org.**Permissions** To request permission to re-use all or part of this article, use this link
<http://cancerres.aacrjournals.org/content/80/17/3606>.
Click on "Request Permissions" which will take you to the Copyright Clearance Center's (CCC) Rightslink site.